Relative stability of amorphous phase versus solid solution in the Ni–Ti system revealed by molecular dynamics simulations

2007 J. Phys.: Condens. Matter 19 046213

(http://iopscience.iop.org/0953-8984/19/4/046213)

INSTITUTE OF PHYSICS PUBLISHING JOURNAL OF PHYSICS: CONDENSED MATTER

J. Phys.: Condens. Matter **19** (2007) 046213 (12pp) doi:10.1088/0953-8984/19/4/046213

Relative stability of amorphous phase versus solid solution in the Ni–Ti system revealed by molecular dynamics simulations

N Gao and W S Lai[1]

Laboratory of Advanced Materials, Department of Materials Science and Engineering, Tsinghua University, Beijing 100084, People's Republic of China

E-mail: wslai@tsinghua.edu.cn

Received 18 August 2006, in final form 10 December 2006
Published 12 January 2007
Online at stacks.iop.org/JPhysCM/19/046213

Abstract

We employ molecular dynamics simulations with n-body potentials to calculate the energies of solid solutions and metallic glasses in the Ni–Ti system to reveal relative stability of two phases against the change of solute concentration. For $Ni_{1-x}Ti_x$ alloys, the calculations show that the energies of the solid solutions are lower than the amorphous phases when $x \leqslant 0.24$ and vice versa for $x > 0.24$, in accord with thermodynamics analysis and experiments. To reveal the underlying physics responsible for this, the evolution of structures in the solid solutions and the amorphous phases are studied via the coordination number (CN) and common neighbour analyses. The results show that, with an increase in Ti concentration, the total average coordination number is close to 12 for all solid solutions owing to the face-centred cubic (fcc) crystalline structure remaining, while it changes from less than 12 to greater than 12 for the amorphous phases, suggesting that more bonds or more fractions of large CNs (>12) exist in the amorphous phases with a high Ti content. The relative stability of the amorphous phases versus the solid solutions revealed by the order of energy is thus correlated with the structural change of the amorphous phases.

1. Introduction

Metallic glass (or amorphous alloy) was first obtained in the Au–Si system by liquid melt quenching (LMQ) in 1960 [1] and since then numerous experimental and theoretical studies have been pursued to investigate one of the basic issues in the field of metallic glasses, i.e. the glass-forming ability of a binary metal system [2, 3]. In practice, a quantitative measure of the glass-forming ability is the glass-forming composition range (GFR), within which amorphous alloys can be obtained via some glass-producing techniques. To produce metallic glass by

[1] Author to whom any correspondence should be addressed.

LMQ, a cooling speed of 10^6 K s^{-1} or even higher is needed to avoid the crystallization of any possible crystalline phases [4]. Generally speaking, by employing LMQ technique, for a given binary metal system, the faster the cooling speed, the broader the GFR. Besides the LMQ technique, other powerful glass-producing techniques were introduced in the early 1980s, such as ion-beam mixing/solid-state reaction of multiple metal layers [5, 6] and mechanical alloying [7]. These techniques have extended not only the GFR, but also the number of glass-forming systems. For instance, some metallic glasses have been obtained in some equilibrium immiscible system, in which LMQ is unable even to obtain any kind of alloys [8]. Many experimental results showed that, with a higher cooling speed (from 10^6–10^9 K s^{-1} in LMQ to 10^{13}–10^{14} K s^{-1} in ion-beam mixing [5]) only metallic glasses and/or simple crystalline phases with face-centred cubic (fcc), body-centred cubic (bcc) or hexagonal close packed (hcp) structures like solid solutions could be obtained, owing to the kinetic frustration of nucleation and growth of equilibrium phases with complicated structures observed in the phase diagram [4].

In theoretical studies, many models have been proposed for predicting the GFR [9–14]. In these models, the main idea for determining the GFR is to consider the competition between terminal solid solutions and amorphous phases, which is based on the experiment results that the GFR has extended to be the whole central composition region, except for terminal solid solutions of two constituent metals for many systems [4]. This led Zhang *et al* to determine the maximum solid solubilities via interatomic potentials as the boundaries within which the central composition region was considered to be the GFR of the binary systems [15]. In thermodynamic models, the GFR was usually determined by comparing the energies of amorphous phases and solid solutions, and amorphous phases were assumed to be formed at the composition region with amorphous enthalpies smaller than those of solid solutions [16]. The results of thermodynamic calculations were compatible with experiments [14, 16].

There have been a lot of experimental results showing that supersaturated solid solutions could be produced by non-equilibrium methods, such as mechanical alloying, ion-beam mixing, etc [4]. For example, ion-beam mixing of Ni–Ti multilayes produced a Ni-rich supersaturated solid solution of 34.94 at.% Ti [17], which is much larger than the equilibrium solubility of ∼7 at.% Ti at room temperature observed from the phase diagram. As the formation of the supersaturated solid solutions will hinder the formation of an amorphous phase, the competition between them thus determines the glass-forming range of a binary metallic system. Even though the Gibb's free energy pertains to thermodynamic equilibrium, many thermodynamic calculations show that it can reveal the relative stability of the amorphous phase versus the supersaturated solid solution, so the results can be used to guide or explain the amorphous phase formation during the non-equilibrium process [14, 16]. However, the information of detailed structures in amorphous phases cannot be given by thermodynamics calculations. Nevertheless, it can be provided by molecular dynamics (MD) simulations. MD simulations have been used for a long time to analyse the atomic structure in metallic glasses, and the atomic structures of amorphous phases from short-range ordering [18, 19] to short-to-medium range ordering [20] have recently been revealed [20–22].

The change in relative stability of the amorphous phase versus the supersaturated solid solution with changing solute composition is believed to relate to atomic structure evolution of the amorphous phase and the solid solution. In this paper, we chose the Ni–Ti system as the subject and calculated the enthalpies of the amorphous phase and the solid solution at different compositions via MD simulations using n-body potentials, especially in the region of Ni-rich supersaturated solid solutions. The atomic configurations of the amorphous phase and the solid solution have been analysed via the coordination number (CN) and common neighbour methods to reveal the relation between structures, composition and energy so that the underlying physics

responsible for the relative stabilities of the amorphous phase versus the solid solution can be unveiled.

2. Simulation method

In the MD simulations, an initial fcc Ni lattice consisting of $8 \times 8 \times 8 \times 4 = 2048$ Ni atoms with periodic boundary conditions applied in all three directions is set for constructing the solid solution and amorphous models. The [100], [010] and [001] crystalline directions are parallel to the x-, y- and z-axes. For the solid solutions, the models are constructed by introducing solute atoms in the fcc Ni lattice through randomly substituting a certain number of Ti atoms for Ni atoms until the desired composition is reached. As the Ni–Ti system has a large negative heat of mixing, the Ni–Ti bonds are readily formed in alloy phases including solid solutions and amorphous phases so as to lower the energy of the system. To maximize the dissimilar bonds in the solid solution as much as possible, random substitution is performed in each unit cell of the Ni fcc lattice with the same probability, and then the initial fcc Ni-rich solid solution is obtained. The solid solution model for each composition is equilibrated at 0 K for 100 ps to reach a state for energetic and structural analysis. For the amorphous states, the models are obtained by heating up the solid solution with the set composition slowly across the liquidus temperature to reach a liquid state and then rapid quenching the liquid to form metallic glasses. The simulations are performed in the following way. First, the liquid is quenched to 10 K by re-scaling the velocity of particles with a speed of 10^{14} K s^{-1}. Second, once the temperature of the system reaches 10 K, the system is kept running at 10 K by re-scaling the velocity at every 100 MD steps for a time of up to 100 ps. A steady state of the system is monitored by the change in energy of the system. The difference in states after running 100 and 200 ps is found to be very small (the relative change in the average energy between two states is less than 10^{-7}), so 100 ps is adopted in our simulations. Finally, the temperature of the system is set to 0 K to further equilibrate the system, so as to obtain the pure enthalpy of an amorphous phase at 0 K. The structures of alloys, including solid solutions and metallic glasses obtained in MD simulations, are analysed using the pair-correlation function and common-neighbour analysis (CNA) to reveal a physical insight into the relative stability of solid solutions versus metallic glasses. The MD simulations are performed with the Parrinello–Rahman constant pressure algorithm [23] (i.e. NTP ensemble: the number of particles N, the temperature T and the pressure P of the system are conserved). with a pressure of $P = 0$ bar, and the equations of motion are integrated with the fourth-order Gear predictor–corrector method [24] with a time step of 1 fs.

The interactions between atoms are described using the tight-binding potentials developed by authors previously [25]. The potentials can reproduce the correct energetic sequence and lattice constants of some intermetallic phases. The amorphization transition via solid-state reaction in the Ni–Ti system was also reproduced by MD simulations [26]. These results suggest that the potentials are well suited for the present simulations.

3. Results and discussion

3.1. General features

Figure 1 displays the total pair-correlation functions, $g(r)$, calculated for the Ni-rich fcc solid solutions and metallic glasses consisting of Ti solute atoms in the range 5–40% obtained with the methods described above. No discrete crystalline peaks are observed in the pair-correlation functions of metallic glasses, indicating amorphous or liquids structures. In contrast, obviously discrete crystalline peaks are visible in the solid solutions, suggesting that their crystalline structures remain. It is well known that the shape of the first peak is a significant sign to show the structure properties [27], and figure 2 shows the decomposition of the first peak for four

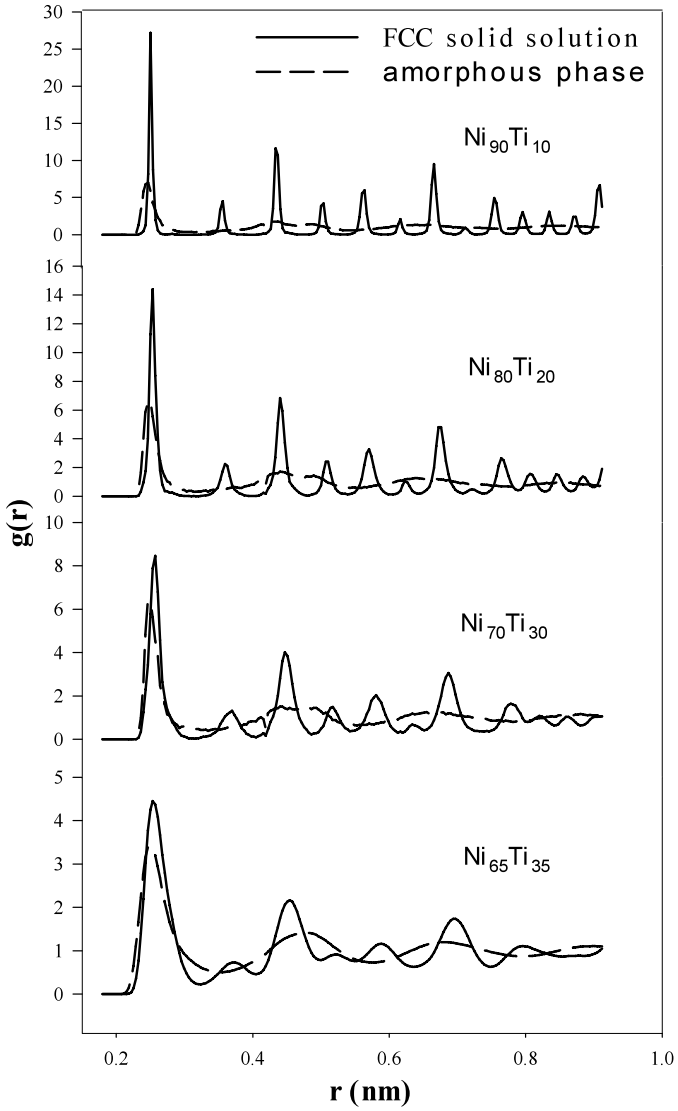

Figure 1. Total pair-correlation functions of the Ni–Ti solid solutions (solid line) and amorphous phases (long dash) for $Ni_{90}Ti_{10}$, $Ni_{60}Ti_{20}$, $Ni_{70}Ti_{30}$, and $Ni_{65}Ti_{35}$.

metallic glasses with different compositions, where the total $g(r)$ is the sum of the partial $g(r)$ of Ni–Ni, Ti–Ti, Ni–Ti and Ti–Ni. It is seen that the shapes of the total $g(r)$ are different and the components of the partial $g(r)$ (i.e. Ni–Ni, Ti–Ti, and Ni–Ti) vary with the change in composition. This suggests that the detailed fine structures of metallic glasses should differ with a variation of their compositions. We will analyse the structures of metallic glasses in detail in section 3.3.

3.2. Calculation of system energy

In the general thermodynamic formulism, the Gibbs free energy of a system is given by

$$G = H - TS \tag{1}$$

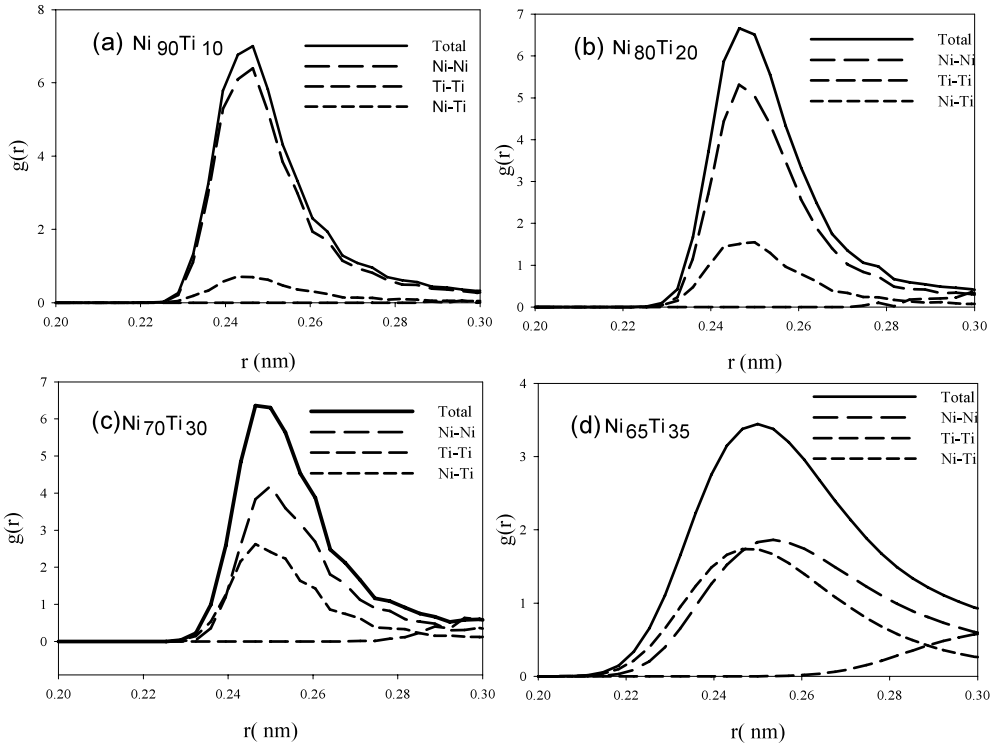

Figure 2. Decomposition of the first peak of total pair-correlation function to partial Ni–Ni, Ni–Ti, Ti–Ni (not shown) and Ti–Ti for four Ni–Ti amorphous phases: (a) $Ni_{90}Ti_{10}$; (b) $Ni_{60}Ti_{20}$ (c) $Ni_{70}Ti_{30}$ and (d) $Ni_{65}Ti_{35}$.

where G, H, S and T are the total Gibbs free energy, enthalpy, entropy and temperature of the system, respectively. At low temperature, the contribution to G comes mainly from H, owing to the contribution of entropy being very small. Here we use the enthalpy of mixing as the metric of stability, so we directly calculate the enthalpies of the amorphous phase and the solid solution at 0 K in the MD simulations. Figure 3 shows the variation in H with composition for the solid solution and amorphous phase in the Ni-rich region for the $Ni_{1-x}Ti_x$ system. It is seen that the energies of both the amorphous phase and solid solution decrease with increasing Ti composition, consistent with a free energy diagram [28] calculated using Miedma's heat of mixing and the regular solution model [29] for the Ni–Ti system at 240 K. Interestingly, it is observed from figure 3 that there is a cross-over point between these two energy curves, and that the energy of the amorphous phase is higher than that of the solid solution when $x \leqslant 0.24$, and vice versa for $x > 0.24$. This result suggests that the amorphous phase is more stable than the solid solution and thus is likely to be formed in a $Ni_{1-x}Ti_x$ alloy with $x > 0.24$. This is in accord with experimental results that the amorphous $Ni_{1-x}Ti_x$ was formed by mechanical alloying [28, 30] for $x \approx 0.25$ and by ion-beam mixing for $x > 0.38$ [17]. In the literature, there are no experimental observations showing that the amorphous phases could be formed for $x \ll 0.25$, whereas the formation of solid solutions in this region was reported [17]. Moreover, the present result is also in agreement with theoretical prediction based on thermodynamic calculations [28, 31]. From the energy curves shown in figure 3, it is seen that the relative stability of the amorphous phase versus the solid solution is related to the compositions of alloys. Looking back at the pair-correlation functions of amorphous phases shown in figure 2,

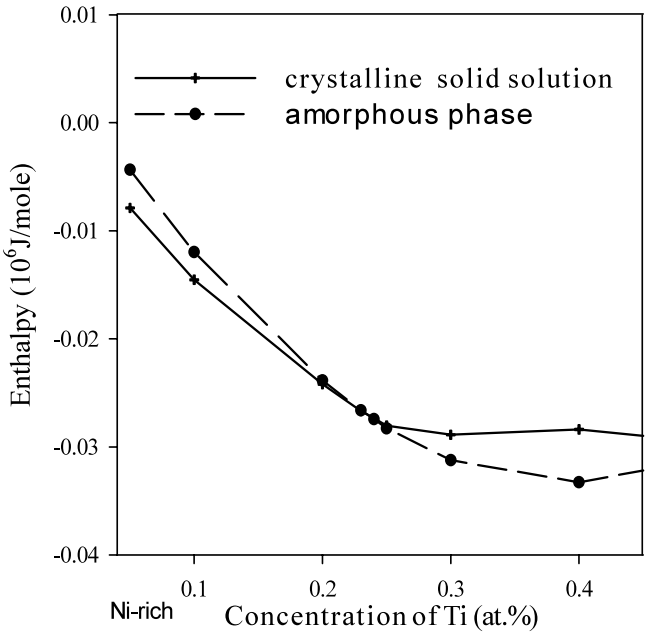

Figure 3. Variation of enthalpy (H) with Ti composition for the solid solutions (solid line) and the amorphous phases (long dash) in the Ni-rich region for the $Ni_{1-x}Ti_x$ system at 0 K.

the shapes of the total $g(r)$ vary with alloy composition, indicating different fine structures for amorphous phases. From the theoretical point of view, the energies of alloys are determined from the atomic configurations with specific structures. Therefore, the relative stability of the amorphous phase versus the solid solution reflects the change of local structure in metallic glasses with changing alloy composition.

3.3. Analyses of coordination number and common-neighbour

In this section, we present the detailed structures of the solid solutions and amorphous states using the coordination number and common-neighbour analysis, so as to reveal the underlying physics responsible for their relative stability. We briefly summarize the methods used and then give the results. The coordination number is obtained by integrating $4\pi r^2\rho_0 g(r)$ up to the first minimum of $g(r)$ shown in figure 1, where ρ_0 is the average atomic density in the model. Common-neighbour analysis (CNA) [34] is a method for analysing structures by decomposition of the radial distribution function (RDF $= 4\pi r^2\rho_0 g(r)$) according to the local environment of the pairs of atoms, and it can provide direct interpretation of various features of the RDF in terms of atomic structure. In the analysis, the first and second peaks of the pair-correlation function represent the first and second nearest neighbours, r_1 and r_2, respectively, and two atoms are defined to be a pair if the distanc between them, r, is within $r_1 < r < r_2$. The pairs are classified by a set of three indices, jkl, which are calculated in the usual way [34]. The first index, j, is the number of neighbours common to both atoms; the second index, k, is the number of bonds between these common neighbours; the third index, l, is the number of bonds in the longest continuous chain formed by the k bonds between common neighbours.

The energy and local structure of an alloy phase is related to CN or the number of bonds of each atom. For the binary alloy systems, Sheng *et al* recently reported that, at the

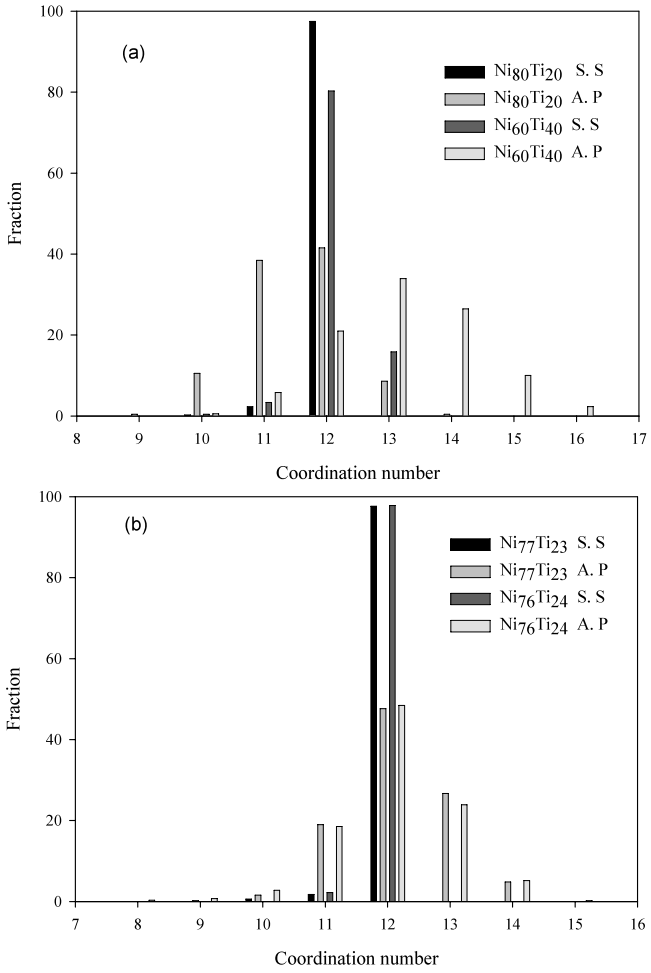

Figure 4. Statistical distributions of coordination numbers for the solid solutions and the amorphous phases: (a) $Ni_{80}Ti_{20}$, $Ni_{60}Ti_{40}$ and (b) $Ni_{77}Ti_{23}$, $Ni_{76}Ti_{24}$.

fixed composition, the CN was not constant and had a statistical distribution in the metallic glass states [20]. In order to find the relation between local structure and CN, the statistical distributions of CNs for solid solutions and metallic glasses of $Ni_{80}Ti_{20}$ and $Ni_{60}Ti_{40}$ are given in figure 4(a). One sees that, for $Ni_{80}Ti_{20}$, the CNs of solid solution include 10, 11 and 12, and the fraction of CN = 12 is dominant; the CNs of the amorphous phase include 9, 10, 11, 12, 13 and 14, and the fractions of CN = 11, 12, 13 are 38.5%, 41.5%, and 8.5%, respectively, compared with 2.3%, 97.4%, 0% in the solid solution. Though the amorphous phase posseses 8.5% large CN of 13, the considerable decrease in the main coordination number (CN = 12) and the increase in the small coordination number (CN = 11) results in an energy higher than that of the solid solution, as seen in figure 3. On the other hand, for $Ni_{60}Ti_{40}$, it is observed from figure 4(a) that the CNs of solid solution include 10, 11, 12, 13 and 14, with the largest fraction of CN = 12 being 80.3% and second fraction of CN = 13 being 15.9%; the CNs of the amorphous phase include 10, 11, 12, 13, 14, 15 and 16, with the dominant fractions of CN = 12, 13, 14, 15 being 20.9%, 33.9%, 26.5%, 10%, respectively. Compared with the

Table 1. Total average coordination number, TCN, calculated for the solid solutions and the amorphous phases of $Ni_{80}Ti_{20}$, $Ni_{76}Ti_{24}$, $Ni_{75}Ti_{25}$ and $Ni_{60}Ti_{40}$.

	TCN			
	$Ni_{80}Ti_{20}$	$Ni_{76}Ti_{24}$	$Ni_{75}Ti_{25}$	$Ni_{60}Ti_{40}$
Solid solution	11.972	12.073	11.954	12.122
Amorphous state	11.486	11.978	11.961	13.192

solid solution, the fraction of CN = 12 in the amorphous phase decreases significantly and the fraction of large CNs (>12) increases greatly. The effect on the energy of the system from increasing the large CNs is greater than that from decreasing the main CN = 12, resulting in the energy of the amorphous phase being lower than that of the solid solution, as observed in figure 3. Thus, the trend of decreasing energy of the system with increasing Ti concentration in figure 3 for the solid solution and the amorphous phase arises from the variation of the CNs and type of bonds with composition. The cohesive energies of fcc Ni, hcp Ti and B2 NiTi are 4.44 eV/atom [32], 4.85 eV/atom [32] and 4.95 eV/atom [33], respectively. As the cohesive energy is mainly contributed by the interaction of the first-nearest-neighbour atoms, we can use the above cohesive energy to estimate roughly the strengths of bonds for Ni–Ni, Ti–Ti and Ni–Ti, which are 0.37, 0.40, and 0.62 eV, respectively. With increasing Ti concentration in the Ni-rich $Ni_{1-x}Ti_x$ alloys, the number of Ni–Ti and Ti–Ti bonds increases, while that of the Ni–Ni bond decreases. This change in the type of bonds results in the decrease in the energy of the system for both solid solutions and amorphous phases, because the bond strengths for Ni–Ti and Ti–Ti are greater than that of Ni–Ni. However, the relative stability of the amorphous phase versus the solid solution may be due to the variation of CNs with composition, because the energy change through increasing a bond (e.g. 0.37 eV for the Ni–Ni bond) is greater than that induced by changing the bond type (e.g. 0.25 eV from Ni–Ni to Ni–Ti bonds). To see how the CNs affect the energy order between the solid solution and the amorphous state near the cross-over point ($x = 0.24$), the statistical distributions of CNs for $Ni_{77}Ti_{23}$ and $Ni_{76}Ti_{24}$ are plotted in figure 4(b). One sees that, for the solid solutions, the main CN of 12 is dominant, owing to their fcc crystalline structure, and that for the amorphous states the profile of CNs broadens, including CNs of 10, 11, 12, 13, and 14. In the amorphous states, the fraction of CN = 12 is almost half that of the solid solutions and the portion for large CNs (>12) is similar to that for small CNs (<12). Thus, the lack of bonds due to the small CNs is compensated by the increment of bonds from the large CNs in the amorphous state. This is the reason why the energy of the amorphous phase is close to that of the solid solution near $x = 0.24$.

To further clarify whether the variation of CNs in the amorphous states does affect the relative stability against the solid solutions, the total average coordination number, TCN, is calculated from

$$\mathrm{TCN} = \sum_{i}^{N} f_i \cdot \mathrm{CN}_i \tag{2}$$

where CN_i is the coordination number of i, and f_i is the fraction of CN_i accordingly. We have calculated TCN for the solid solutions and metallic glasses of $Ni_{80}Ti_{20}$, $Ni_{76}Ti_{24}$, $Ni_{75}Ti_{25}$ and $Ni_{60}Ti_{40}$, and the results are listed in table 1. One sees that TCN for all solid solutions are close to 12 owing to the crystalline structure remaining, while TCN for the amorphous phases fluctuates around 12. It is seen from table 1 that the TCN increase with an increase in Ti content for both the solid solutions and the amorphous phases, with the exception of $Ni_{75}Ti_{25}$, which may be due to statistical error. The greater the TCN of a system is, the lower the energy of the

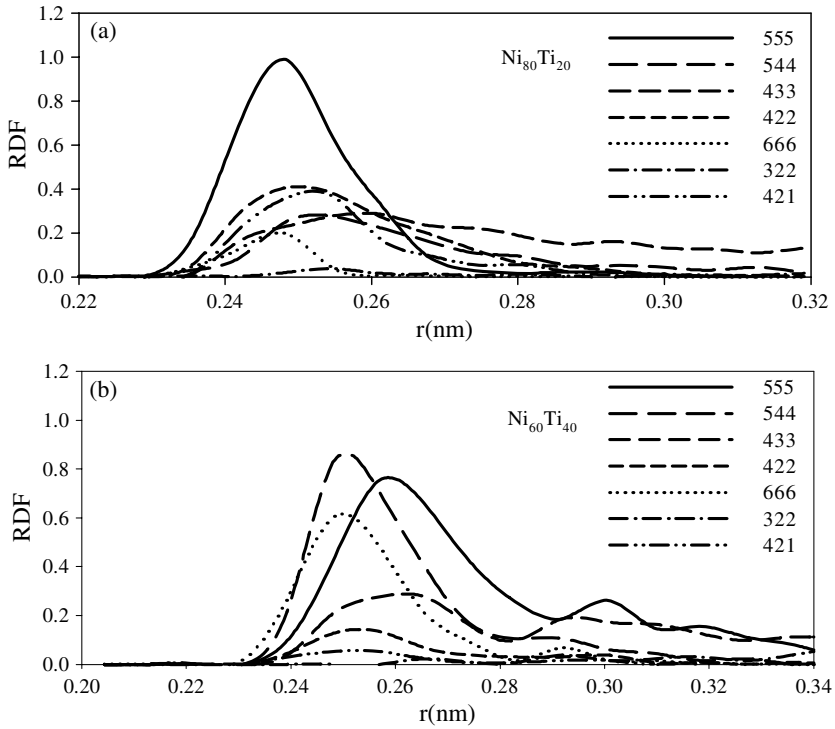

Figure 5. Common-neighbour analysis of radial distribution function (RDF) for the amorphous phases: (a) $Ni_{80}Ti_{20}$ and (b) $Ni_{60}Ti_{40}$.

system becomes. Thus the energies of the amorphous phases decrease with increasing TCN. The tendency of increasing TCN in the range $0.1 < x < 0.4$ agrees with the tendency of the drop in energy curves, though the fluctuation of local compositions in the amorphous phases may also have an impact on the energy curves. Therefore, it is concluded that the large increase in the large CNs (>12) in the amorphous phase with increasing Ti concentration results in a faster decrease in energy of the system than for the solid solution.

We now turn to common neighbour analysis. Figure 5 gives the CNA for metallic glasses $Ni_{80}Ti_{20}$ and $Ni_{60}Ti_{40}$, and figure 6 shows the statistical distributions for various indices jkl in the metallic glasses. It is clearly seen that, as the content of Ti changes from 20% to 40%, the fraction with indices 555 (representing an icosahedron) changes a little, but those of 666 and 444 (mostly found in the crystalline bcc structure) increase remarkably, while those of 421 and 422 (mostly found in the crystalline fcc structure) decrease considerably. The indices 555, 543 and 433 are often found in the undercooled liquids or glasses, such as in the Ni–Ti metallic glasses studied here. The above results suggest that, at low Ti content, the Ni–Ti amorphous structure features an icosahedron and some fcc-like local structure, while at high Ti content, the amorphous phase features an icosahedron and some deformed bcc structure which draws the second neighbours of bcc into the first neighbours, forming an icositetrahedron. Recently, Tai *et al* found structural development with Ag content in the Ag–Nb system, and the icositetrahedron had been viewed in the metallic glasses [35]. It is also seen from figure 6 that, on increasing the solute atoms, the high indices (such as 666, 555, 444) increase while the low indices (such as 421, 422) decrease, suggesting that the number of bonds (or CNs) of the system increases on increasing the solute atoms.

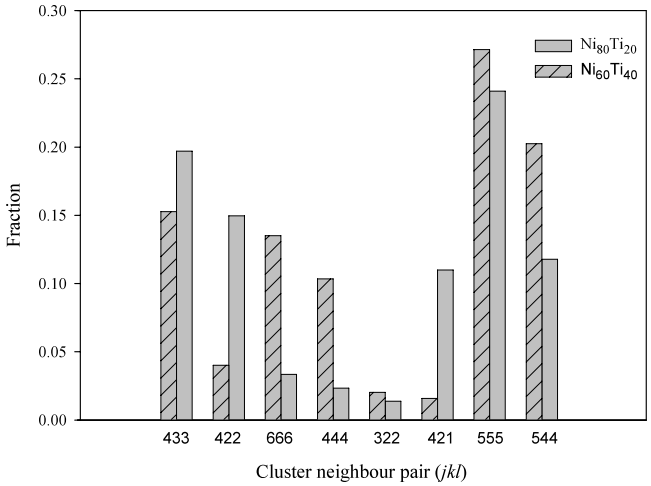

Figure 6. Statistical distributions for each type j, k, l in $Ni_{80}Ti_{20}$ and $Ni_{60}Ti_{40}$ amorphous phases.

3.4. Validation of relative stability by annealing simulation

To demonstrate the relative stability of solid solution versus metallic glass further, we perform an annealing experiment in MD simulation for $Ni_{65}Ti_{35}$. It should be mentioned that the nominal GFR of the Ni–Ti system observed by liquid melt quenching was in a composition range of 30-40 at.% Ni [14]. The GFR of the Ni–Ti system determined by other experiments and theoretical predictions is from 15 to 62 at.% Ni [15]. In order to reveal the relative stability, we chose the composition $Ni_{65}Ti_{35}$, which is outside the range of the previous theoretical predictions but inside the range of the energy curve shown in figure 3. The solid solution has been obtained using the random substitute method described in section 2. The temperature for the solid solution simulation is set to 300 K and kept for running up to 100 ps as an initial state. The temperature range for the annealing experiment of the simulation is chosen to be from 300 to 800 K. From the initial state, the system is heated up at a rate of 10^{14} K s^{-1} to a desired temperature and then kept annealing at that temperature. When the temperature of the system reaches 700 K, an amorphization transformation occurs. The state of the amorphous phase is obtained by keeping running for 100 ps to get rid of any memory of the system. Figure 7 shows the pair-correlation functions of the solid solution and the amorphous phase obtained at 300 and 700 K, respectively. It is clearly seen that, when the temperature is at 300 K, the state of the system remains the solid solution. However, when the temperature reaches 700 K, the state of the system transforms from the solid solution to the amorphous phase. The results of the annealing experiments confirm that the amorphous phase is more stable than the solid solution for $Ni_{65}Ti_{35}$, which is in agreement with the energy curve.

4. Conclusions

The relative stability of solid solutions versus metallic glasses in the Ni–Ti system is studied by MD simulations with n-body potentials by calculating the energy change with increasing Ti concentration. The results show that, for the Ni-rich $Ni_{1-x}Ti_x$ alloys, the energies of the solid solutions are lower than those of metallic glasses when $x \leqslant 0.24$, and vice versa for $x > 0.24$. It is known that the amorphous state is likely to be obtained in the composition range where the

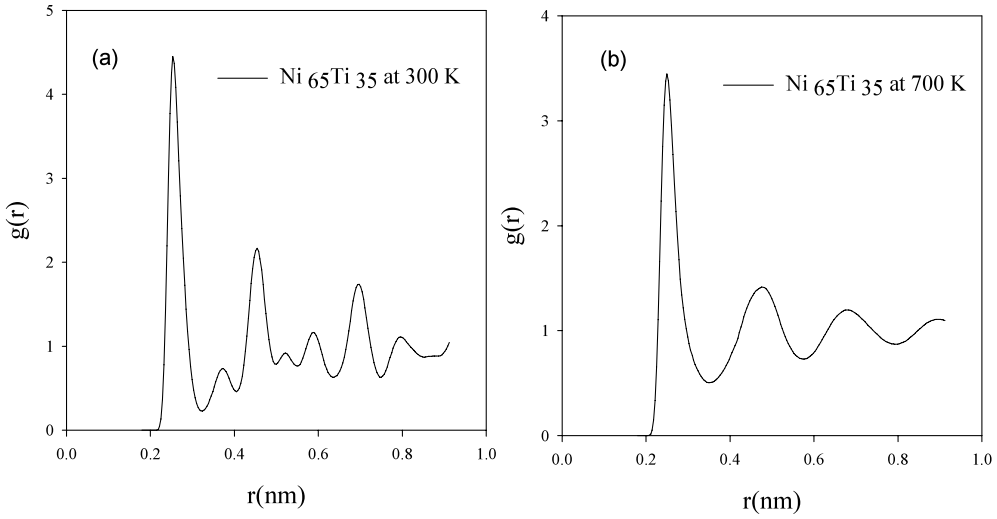

Figure 7. The pair-correlation functions of $Ni_{65}Ti_{35}$ alloy: (a) the solid solution obtained at 300 K and (b) the amorphous phase obtained at 700 K.

energy of the amorphous phase is lower than that of the competing solid solution. Therefore, the glass-forming range can be predicted from the relative stability of the two competing phases, and the present result for $Ni_{1-x}Ti_x$ with $x > 0.24$ is consistent with the experimental results.

The structural evolution with increasing solute content is studied in detail for the solid solutions and the metallic glasses through analysing the coordination numbers and the common-neighbour atoms. It is shown that with an increase in Ti concentration, the total average coordination number is close to 12 for all solid solutions owing to their fcc crystalline structure, while it changes from less than 12 to greater than 12 for the metallic glasses. The common-neighbour analysis unveils that the fractions of high indices (such as 666 and 555) with more common neighbours and long chains of bonds increase in metallic glasses with increasing Ti concentration. This suggests that more bonds or more fractions of large CNs (>12) exist in metallic glasses with high Ti content, resulting in the energy of the system being lower than for the solid solutions. It is therefore concluded that the relative stability of the solid solutions versus the metallic glasses revealed by the order of energy is correlated with the evolution of local structures of the metallic glasses.

Acknowledgments

This work is supported by the National Natural Science Foundation of China (grant nos. 50471010 and 50531040) and the Program for New Century Excellent Talents in University, the Ministry of Education of China.

References

[1] Duwez P, Willens R H and Klement W 1960 *J. Appl. Phys.* **31** 1136
[2] Ruhl R C, Giessen B C, Cohen M and Grant N J 1967 *Acta Metall.* **15** 1693
[3] Poon S J and Carter W L 1980 *Solid State Commun.* **35** 249
[4] Liu B X, Lai W S and Zhang Q 2000 *Mater. Sci. Eng. Rep.* **29** 1
[5] Liu B X, Johnson W L, Nicolet M-A and Lau S S 1983 *Appl. Phys. Lett.* **42** 45

[6] Schwarz R B and Johnson W L 1983 *Phys. Rev. Lett.* **51** 415
[7] Koch C C *et al* 1983 *Appl. Phys. Lett.* **43** 1017
[8] Liu B X, Ma E, Li J and Huang L J 1987 *Nucl. Instrum. Methods Phys. Res.* B **19/20** 682
[9] Liu B X, Lai W S and Zhang Q 2000 *Mater. Sci. Eng. Rep.* **29** 1
[10] Egami T 1996 *J. Non-Cryst. Solids* **205–207** 575
[11] Kaufman L 1978 *CALPHAD* **2** 117
[12] Murray J L 1983 *Bull. Alloy Phase Diagrams* **4** 81
[13] Saunders N 1985 *CALPHAD* **9** 297
[14] Schwarz R B, Nash P and Turnbull D 1987 *J. Mater. Res.* **2** 456
[15] Zhang Q, Lai W S and Liu B X 1999 *Phys. Rev.* B **59** 13521
[16] Takeuchi A and Inoue A 2001 *Mater. Trans. JIM* **42** 1435
[17] Lai W S, Li Q, Lin C and Liu B X 2001 *Phys. Status Solidi* b **227** 503
[18] Bernal J D 1960 *Nature* **185** 68
[19] Bernal J D 1964 *Proc. R. Soc.* A **280** 299
[20] Sheng H W, Luo W K, Alamgir F M, Bai J M and Ma E 2006 *Nature* **439** 419
[21] He J H, Sheng H W, Schilling P J, Chien C-L and Ma E 2001 *Phys. Rev. Lett.* **86** 2826
[22] Hufnagel T C 2004 *Nat. Mater.* **3** 666
[23] Parrinello M and Rahman A 1980 *Phys. Rev. Lett.* **45** 1196
[24] Allen M P and Tildesley D J 1987 *Computer Simulation of Liquids* (New York: Oxford University Press)
[25] Lai W S and Liu B X 2000 *J. Phys.: Condens. Matter* **12** 53
[26] Lai W S, Zhang Q, Liu B X and Ma E 2000 *J. Phys. Soc. Japan* **69** 2923
[27] He J H and Ma E 2001 *Phys. Rev.* B **64** 144206
[28] Schwarz R B 1988 *Mater. Sci. Eng.* **97** 71
[29] Miedma A R 1976 *Philips Tech. Rev.* **36** 217
[30] Schwarz R B, Petrich R R and Saw C K 1985 *J. Non-Cryst. Solids* **76** 281
[31] Gallego L J, Somoza J A, Alonso J A and López J M 1988 *J. Phys. F: Met. Phys.* **18** 2149
[32] Kittel C 1986 *Introduction to Solid Physics* (New York: Wiley–Interscience)
[33] Hultgren R, Desai P D, Hawkins D T, Gleiser M and Kelly K K 1973 *Selected Values of Thermodynamics Properties of Binary Alloy* (Metals Park, OH: ASM International)
[34] Faken D and Jónsson H 1994 *Comput. Mater. Sci.* **2** 279
[35] Tai K P, Gao N, Li J H, Lai W S and Liu B X 2006 *Appl. Phys. Lett.* **89** 094108